

Coarse grained description of the protein folding

Marek Cieplak and Trinh Xuan Hoang

Institute of Physics, Polish Academy of Sciences, 02-668 Warsaw, Poland

We consider two- and three-dimensional lattice models of proteins which were characterized previously. We coarse grain their folding dynamics by reducing it to transitions between effective states. We consider two methods of selection of the effective states. The first method is based on the steepest descent mapping of states to underlying local energy minima and the other involves an additional projection to maximally compact conformations. Both methods generate connectivity patterns that allow to distinguish between the good and bad folders. Connectivity graphs corresponding to the folding funnel have few loops and are thus tree-like. The Arrhenius law for the median folding time of a 16-monomer sequence is established and the corresponding barrier is related to easily identifiable kinetic trap states.

PACS numbers: 87.15.By, 87.10.+e

Proteins that are found in nature are special sequences of aminoacids that fold rapidly into their native states under physiological conditions [1]. The native states control functionality of proteins and are commonly assumed to coincide with the ground state conformations. Exploration of the protein's phase space in search of the native state typically takes milliseconds. This is in contrast to an essentially indefinite search expected for randomly constructed sequences of aminoacids – such sequences are generally bad folders. It is believed that the well folding biological sequences have an energy landscape with a dominating folding funnel which restricts the number of visited conformations during folding. Based on simulations of lattice models, Onuchic et al. [2] have identified the crucial landmarks in the folding funnel such as the molten globule states and low energy bottlenecks. Before, Leopold et al. [3] have studied transition rates between conformations found in the last stages of folding and interpreted the resulting trajectories as forming a folding funnel. In this paper, we focus on ways to define folding funnels operationally, in numerical simulations. We consider two- and three-dimensional lattice models, the dynamics of which are given as a Monte Carlo process with single and two monomer moves.

The point of view that we propose here is that the Monte Carlo dynamics generates too many states, each of an overall negligible occupancy, to allow for a convincing and easy to do identification of the funnel without some educated organization of the data. Thus some reduction in the description should facilitate the task by an elimination of conformations that are less relevant. A valid analogy here is with a solid: understanding properties of a solid can often be reached from knowledge of the crystal structure in the ground state without taking into account any phonon states. Stillinger and Weber [4], in the context of glasses, and Cieplak and Jaeckle [5], in the context of spin glasses, have accomplished a useful elimination of such 'phonon' states by mapping states of a system to underlying local energy minima obtained, in a unique way, through the steepest descent

method. The motion of the system through the phase space could then be viewed as an effective migration between the underlying 'valleys'. This approach has been subsequently adopted to proteins by Cieplak, Vishveshwara, and Banavar [6] and by Cieplak and Banavar [7]. It has been implemented for two-dimensional 16-monomer lattice models. The procedure consisted of a two-stage mapping: first an encountered conformation was mapped to a local energy minimum (LM) through the steepest descent method and then the LM was mapped to a nearest maximally compact conformation, called 'cell' for short, defined as one which has maximum energy overlap in common contacts between LM and the cell. If several cells satisfy this criterion, the one with the lowest total energy is picked.

This particular scheme of coarse graining of the protein dynamics has been successful since the resulting pattern of connectivities between frequently occupied cells was clearly differentiating between the bad and good folders and, in the latter case, was showing emergence of a funnel. It has turned out, however, that the approach based on cells is difficult to implement for longer polymers, especially in three dimensions. For instance, for a 27-monomer lattice model, there are 103346 maximally compact $3 \times 3 \times 3$ cells and it is hard to find a fast way to tell which of them is the closest to an LM. An alternative to the criterion of maximum energy overlap is a mapping to a cell which is the easiest to be reached kinetically but finding a reasonable algorithm for this has turned out to be even harder. More importantly, as we shall see here, the connectivity patterns usually are not sensitive enough to allow for a detection of truly relevant trapping states.

In this paper, we discuss a coarse graining scheme that is based on the LM's instead on the cells. Since the LM's are much more abundant than cells it might seem that the technical problems compound. What makes the scheme tractable, however, is that we do not consider all LM's that the system is endowed with, but only those which have been encountered. In addition, this allows for a

more detailed characterization of funnels.

We start, in Section 2, by considering two 12-monomer sequences, A and B, the dynamics of which have been recently studied in two dimensions by an exact solution of the master equation [8]. The properties of these sequences are then very well understood and, in particular, the kinetic traps that govern the long time dynamical behavior at low temperatures, T , have been identified. A is a good folder whereas B is a bad one and we demonstrate that the pattern of connectivities between LM's into which the states of the system have been mapped to yields a funnel for A but not for B. In Section 3, we consider two 16-monomer sequences in two dimensions, R and DSKS' of references [6,7] – again the good and bad folder respectively, and compare the LM-based dynamics to the cell-based dynamics. Finally, in Section 4, we present results for one good folder in 3 dimensions.

The energy of all of these sequences is given by

$$E = \sum_{i < j} B_{i,j} \Delta(i - j) , \quad (1)$$

where $\Delta(i - j)$ means that the monomers i and j form a contact, i.e. they are nearest neighbors on a lattice but are not neighbors along the sequence. $B_{i,j}$ are the corresponding contact energies – essentially the numbers generated with the Gaussian probability distribution but with a mean shifted to negative values to provide compactness in the ground state. The equilibrium properties of the sequences may be characterized by a folding temperature, T_f . Following [9] we define T_f as T at which the equilibrium probability to find the system in the native state crosses $\frac{1}{2}$. A large value of T_f signifies substantial thermodynamic stability which good folders are expected to possess. Temperature scales that characterize dynamics can be determined from the plot of the median folding time, t_{fold} versus T : T_{min} is where t_{fold} achieves a minimum and T_g , the glass temperature, is a low temperature point at which t_{fold} becomes steep. The definition of T_g depends on adoption of a cut-off time that is considered to be too long whereas T_{min} , corresponding to the fastest folding, is criterion-independent. For good folders T_f is comparable to T_{min} . For bad folders T_f is much smaller than T_{min} and then the system becomes trapped in a non-native state at low temperatures before acquiring any substantial stability of the native state. The characterization of the two-dimensional sequences studied here has been given before and we focus only on the coarse-grained kinetics.

The Monte Carlo process starts from a random self-avoiding walk and it has the move sets of Figure 1a and case (i) of Figure 1b in reference [10]. The single monomer moves have an a priori probability of 0.2 and two monomer moves that of 0.8. This process is performed in such a way that the detailed balance condition is satisfied [8,10], i.e. besides the energetics, the probability to perform a move depends on how many kinetic possibilities are allowed in a given conformation, com-

pared to the maximum number of possibilities of $N + 2$, where N is the number of monomers in a sequence.

I. 12-MONOMER SEQUENCES IN TWO DIMENSIONS

The $N=12$ sequences A and B are defined in reference [8]. Both can exist in 15037 conformations out of which 31 are 2×3 cells. Sequence A has the native state, of energy -11.5031, which has an appearance of the letter S. Altogether, the sequence has 495 LM's out of which 403 are V-shaped, i.e., any move out of them costs an energy increase, and 92 U-shaped, i.e. some moves leave the energy unchanged. All states in an U-shaped minimum count as one in what follows. Sequence B has a doubly degenerate native state of energy -8.7675 – both states count together when considering folding; none of the states in the doublet is maximally compact. Among the 496 LM's, 400 are V-shaped and 96 are U-shaped. T_f and T_{min} for sequence A are comparable since they are around 0.7 and 1 respectively. For the bad folder B, on the other hand, T_{min} is again around 1 but T_f is 0.01. We compare dynamics of the two sequences at two temperatures: 1 and 0.4. For sequence A, t_{fold} at these two temperatures is 2 052 and 36 022 respectively and for sequence B it is 2 457 and 215 364, as obtained by studying 500 different trajectories.

Figure 1 shows energy in a segment of a Monte Carlo trajectory for A at $T=1$ and compares it to energies obtained by the one- and two -stage mapping to the LM's and cells respectively. This temperature corresponds to the fastest folding. Naturally, the higher level of coarse-graining, the smoother the dependence of the effective energy on time. For both methods of coarse-graining, the native state appears to have substantial occupancy even though the sequence has not folded yet. It is thus clear that the system moves pretty much in the native valley which is easy to detect if one removes the 'spurious' states from the description.

Figure 2 shows P_0 , L_0 , and C_0 versus T for sequence A. The first of these parameters is the equilibrium probability to find the native state. The second is the probability to find the native state after mapping to the local energy minima. Finally, the third is the probability to find the native state after mapping to the cell states. We see that the cell dynamics enhances the role of the native cell much more significantly than the LM-based dynamics and the maximum C_0 for the good folder is about 3 times as large as for the bad folder. The maximum in C_0 is closer to T_f whereas the maximum in L_0 is closer to T_{min} .

All states of the system, local energy minima or not, can be enumerated and their occupancies can be monitored. Figure 3 shows occupancies of states found during folding on 500 Monte Carlo trajectories for sequence A and compares them to occupancies of LM's obtained

by the one-stage mapping. At T_{min} , local energy minima on the trajectories count overall as much as other states. In the low energy part of the spectrum, however, the LM's dominate heavily. At low temperatures, on the other hand, the time spent in states which are not minima is negligible. Furthermore, certain LM's become heavily populated. The biggest occupancy belongs to the state, denoted as TRAP, which is the most potent kinetic trap on the way to folding. This is the same state which has been identified in reference [8] as contributing most heavily to the eigenmode corresponding to the longest relaxation time. Thus identification of the kinetic traps does not need to involve diagonalization of the master equation – this task can be accomplished by counting occupancies of states encountered in the Monte Carlo. The trap state is also substantially represented after mapping all states to LM's through the steepest descent procedure.

When the trajectories are not terminated at folding but are continued long enough (of order 1 million steps) to see equilibrium values of P_0 , the occupancy of the trap state drops from about 25%, at $T=0.4$, to about 3% – both before and after the mapping,

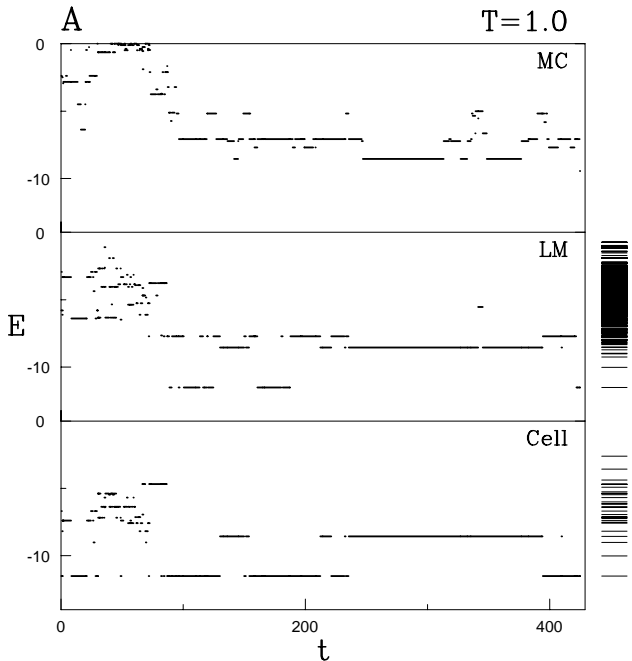


FIG. 1. Top: Energy of states versus number of the Monte Carlo steps in a 424-step long segment of one trajectory for sequence A. Middle: Energy of the local energy minima versus the Monte Carlo time. The minima were obtained by the steepest descent quenching from the states at the top. The energy spectrum of the minima is shown on the right. Bottom: Energy of the maximally compact states, obtained by mapping the LM's from the middle panel, versus the Monte Carlo time. The energy spectrum of the cells is shown on the right.

For sequence B, local energy minima on the trajectories count overall less than for A but, like for A, the proportions in equilibrium remain similar to those found in the folding stage. A trap state for sequence B, however, has a more substantial representation in equilibrium: it accounts for 9% on trajectories and 17% after the steepest descent quenching. This trap state has been discussed in reference [8]. Here, it is enough to mention that going from the trap state of sequence B to the native state requires full unfolding so this state forms a valley which is competing with the native valley. For sequence A, on the other hand, the most important trap is in the native valley and reaching the native state from this trap requires only partial unfolding.

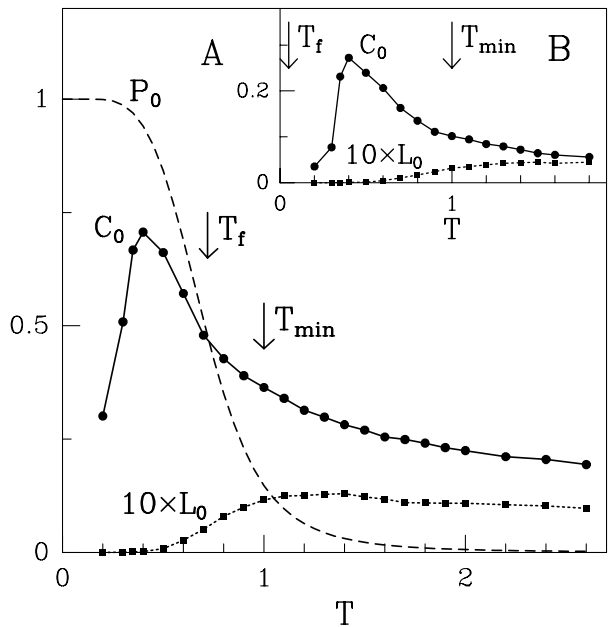


FIG. 2. Probability to find the native state before any mapping, P_0 , after one-stage mapping, L_0 , and two-stage mapping C_0 , as explained in the text. The main figure is for sequence A and the inset for B. The values of T_{min} and T_f are indicated.

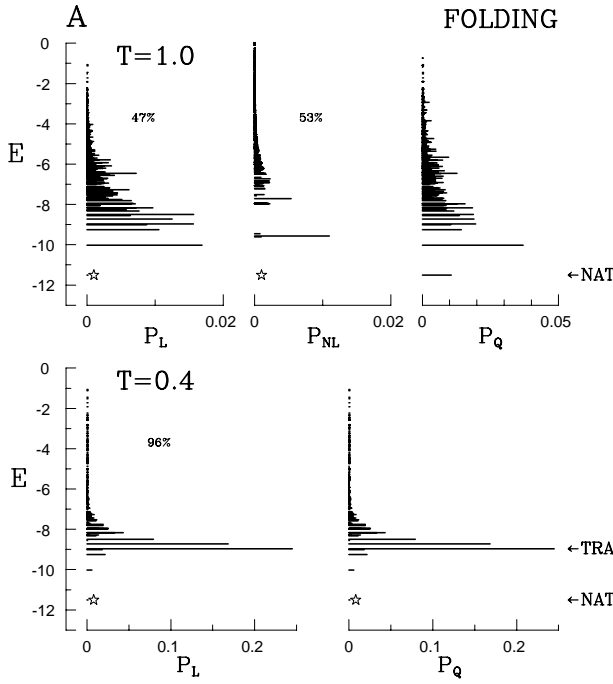


FIG. 3. Occupancy histograms for A based on 500 Monte Carlo trajectories that were terminated at folding. The asterisk marks the energy of the native state. The top panels are for $T=1$ and the bottom panels for $T=0.4$. P_L and P_{NL} denote probabilities to find respectively LM's and states which are not LM's in the Monte Carlo trajectories. The numbers shown indicate integrated probabilities. P_Q denotes probability to find an LM after the steepest descent quenching. The trap state accounts for about 1/4 of the total time both before and after mapping to LM's. For sequence B, the integrated occupancies at $T=1$ are 39% and 61% for P_L and P_{NL} respectively. At $T=0.4$ the integrated P_L is 77%.

Cell dynamics

We now proceed to the various ways to represent dynamics in the coarse grained sense. We begin by discussing the description which is the most economical in presentation and the one that has been proposed in references [6,7]. This is the description based on the two-stage mapping to cells, i.e. corresponding to the bottom of Figure 1. When the system leaves one cell and arrives at another a connection between the two cells is established. We count such connectivities in 500 trajectories which terminate at folding and average to get connectivities. The connectivities can be represented in a matrix form. The matrix is, in principle, 31×31 and it is symmetric. Most of the connectivities are weak or absent and a reduced matrix, by adopting a cutoff, describes the dynamics adequately. This is shown in Figure 4 which compares the dynamical matrix at T_{min} and at a low temperature. It is seen that the good folder at the most favorite folding conditions generates a matrix which involves many direct connections to the native cell. The folding funnel, in this description, consists of the cells

which are connected to the native cell. At low temperatures, and also for the bad folder B at any temperature, the matrix looks more like the bottom panel of Figure 4: there are much fewer direct connections of the low energy cells to the native cell, some connections become multiple step, or all connections correspond to higher energy motions that are not connected to the native cell (this last mode, however, is not seen in Figure 4 since the system is too small). Finally, it should be pointed out that the cell dynamics does not differentiate between the native cell and the trap state, because the cell which is the closest to the trap happens to actually coincide with the native cell for both sequences studied here.

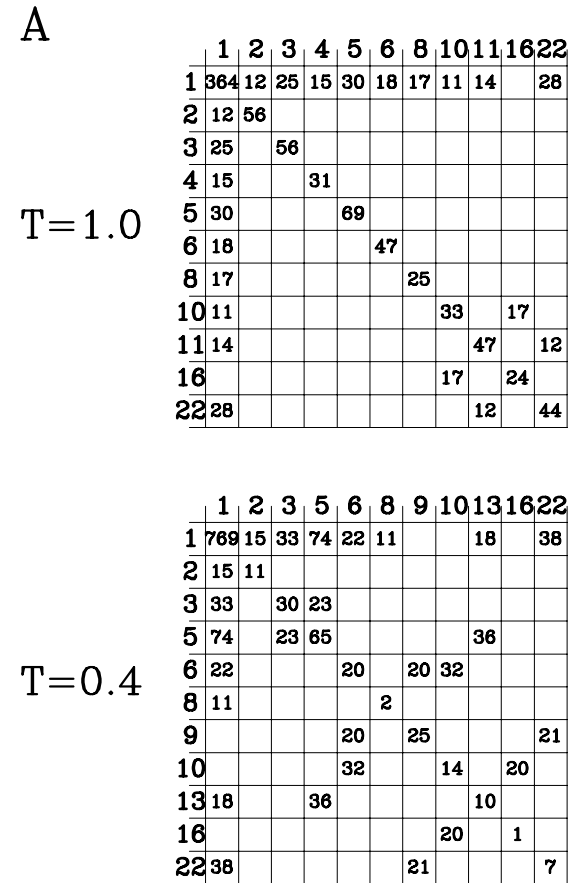


FIG. 4. Cell-to-cell connectivities for sequence A and temperatures indicated. The cell labels correspond to the energy-wise rank ordering. Cell number 1 is thus native. The connectivities are normalized to 1000 and only those larger than 10 are shown. The diagonal terms indicate similarly normalized values of the cell occupancies.

Dynamics based on the local energy minima

Consider now the one-stage mapping. The connectivities are now determined between the LM's as shown in the middle panel of Figure 1. A matrix representation of the results becomes impractical since too many states are involved. Instead we opted for the graphical representa-

tion as shown in Figures 5 and 6 for sequences A and B respectively. In these figures, the vertical axis corresponds to energy. The positions of LM's in the horizontal direction are chosen according to two criteria: 1) the lines connecting them overlap as little as possible, 2) the states corresponding to different clusters are shown separately (the cluster analysis depends on the connectivity cutoff). The x-axis coordinate is thus the conformation number, N_c , of the local minimum. The labelling of the minima is well defined and it is based on a computer generated listing. The graphical horizontal placement of the LM on the figure, however, is subjective and it is arranged in a way that demonstrates the divisions into clusters of connectivities. This subjectivness is due to the fact that we adopt a 2D projection. In a many-dimensional space of the conformation labels, the connectivity lines have an objective meaning. The thickness of lines connecting the LM's is proportional to the frequency of the appearance of the connection and the symbols corresponding to the LM's have sizes controlled by probability to find these states.

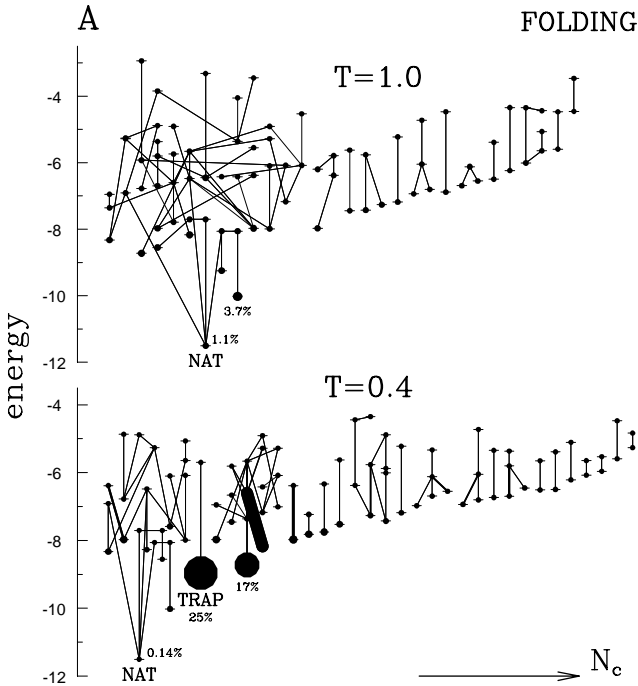


FIG. 5. Connectivities between the local energy minima for sequence A during folding. The connectivities are normalized to 1 and only those exceeding 0.001 are shown – a full description would involve 495 LM's. For $T=1$ and 0.4 the connectivities displayed add up to 24% and 73% of all connectivities. The thickness of the connecting line indicates the magnitude of connectivity. The size of the circle that locates an LM indicates its occupancy after quenching – an analog of the diagonal element in the matrix in Figure 4. The small print numbers shown indicate the occupancy of the corresponding LM. NAT indicates the native LM and TRAP indicates the low temperature kinetic trap.

For the good folder, a well developed knot of states connected to the native state is seen, in Figure 5, both at low temperatures and at those which are good for folding. We interpret this knot as the folding funnel. In addition, other knots of relevant inter-valley motions are also present – the dynamics is indeed dominated by the funnel but it is not restricted to it. At $T=1$, the trap state does not contribute to the effective dynamics. It does contribute at $T=0.4$, however, but – within the cutoff adopted here – it is not connected to the funnel.

The graph of connectivities for the bad folder, shown in Figure 6, indicates a much smaller knot connected to the native LM and no connections to the native LM at the lower temperature. All knots that are present are at elevated energy states. Thus this graphic representation clearly distinguishes between good and bad folders.

Figure 7 is again for the good folder. It shows the graph of connectivities at conditions of equilibrium, i.e. well past folding. Again, the native LM plays the dominant role. Furthermore, at low T 's the dynamics consists primarily of transitions between the native state and a nearby LM which is not the state which provides the most of kinetic trapping during folding at low T 's.

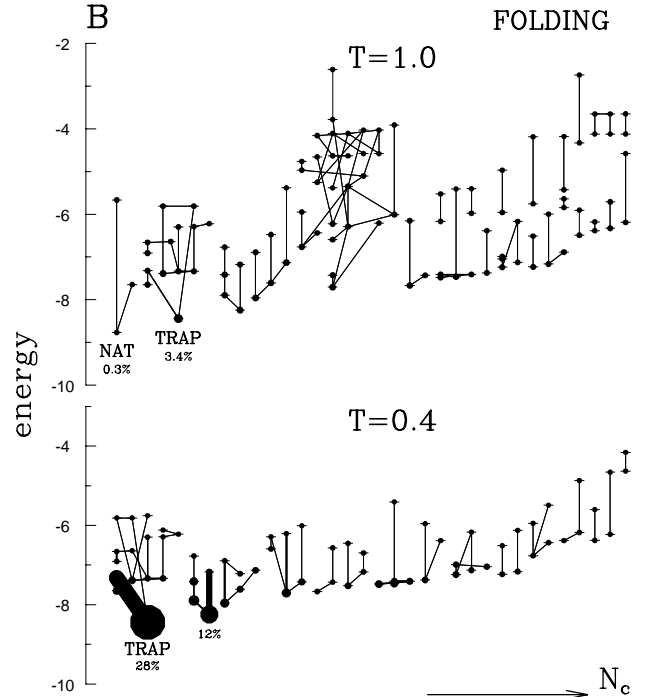


FIG. 6. Similar to Figure 5 but for sequence B. Respectively, 24% and 85% of all connectivities for $T=1$ and 0.4 are displayed.

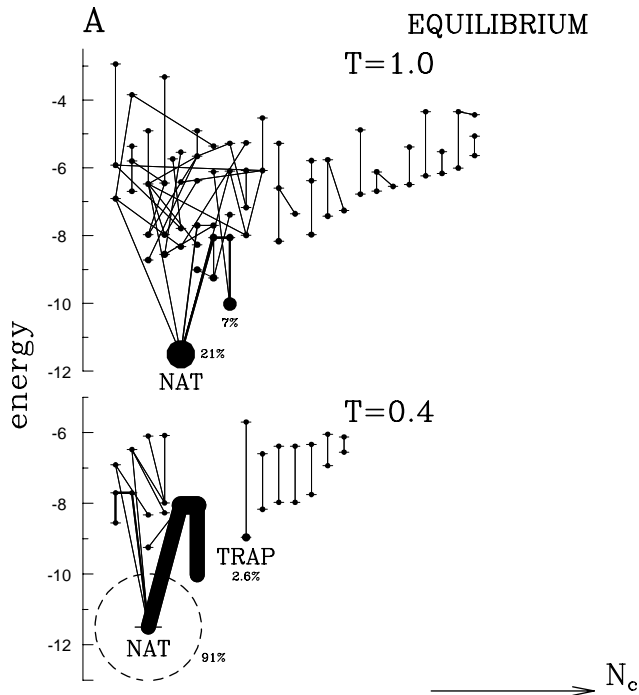


FIG. 7. Similar to Figure 5, and also for sequence A, but in equilibrium – when the trajectories are continued after folding (31% of connections at $T=1$ and 94% at $T=0.4$). For sequence B, the graph in equilibrium is close to the one corresponding to folding.

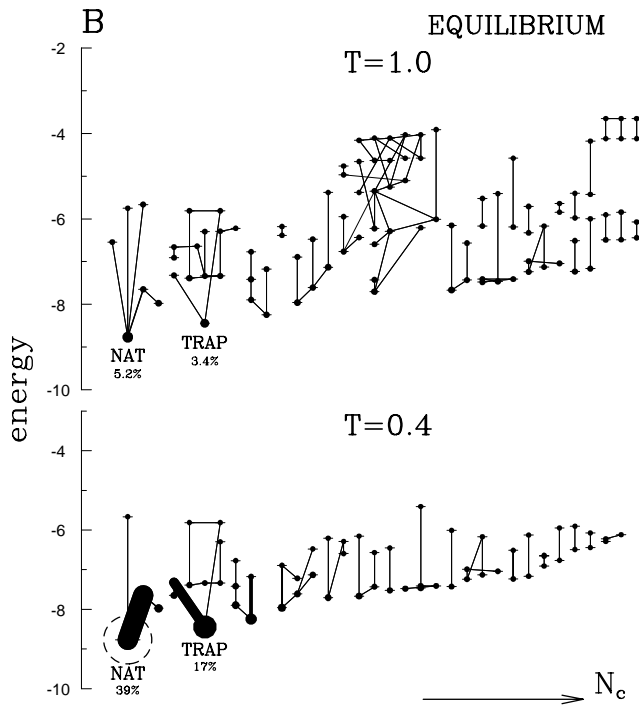


FIG. 8. Similar to Figure 7 but for sequence B.

Figure 8 shows the equilibrium graph of connectivities for sequence B. It clearly shows two, essentially equivalent

but disconnected knots one related to the native state and the other to the trap state. The system then ‘lives’ essentially in these two valleys, which is consistent with our understanding of the physics characterizing this sequence: for sequence B, the native state can be reached from the trap state only through a full unfolding.

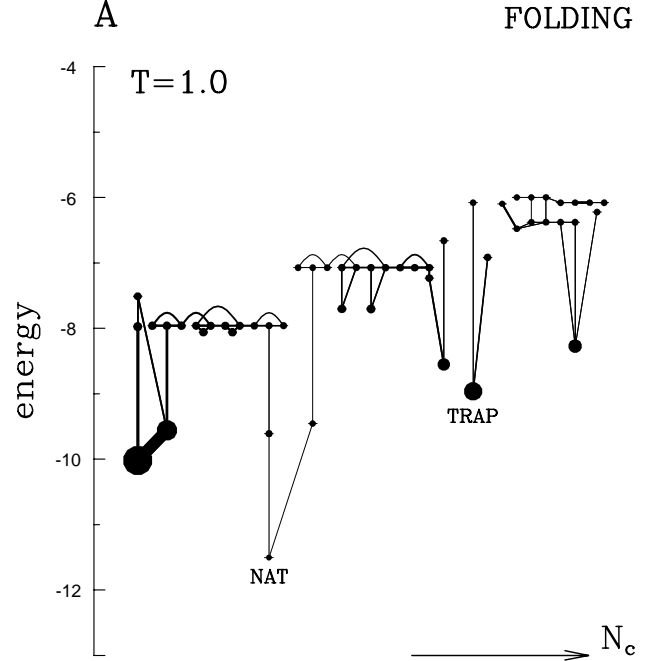


FIG. 9. Graph of connectivities between states on the Monte Carlo trajectory for sequence A for the folding stage. The figure is based on 500 trajectories. There are many clusters and 3 of the most relevant ones are displayed here. The native cluster consist of 34 states and the second biggest cluster of 15 states. 1000 of the most populated states, out of 15037, were monitored and the connectivity cutoff was 0.0002 of all monitored connectivities.

The overall look of the graphs shown in Figures 5-8 is that of *trees*, i.e. the graphs show very few loops. This is not so when one does not map the Monte Carlo states into local minima but just monitors connectivities between the original states. In this case, many knots with loops develop and an example of this is shown in Figure 9. This method of monitoring the dynamics is not practical even for the 12-monomer system due to the sheer number of possible connections.

II. 16-MONOMER SEQUENCES IN TWO DIMENSIONS

We now come to more complex sequences. Following reference [6,7] we consider 16-monomer sequences which have 802 075 conformations, of which 69 are cells. We focus on two sequences: R and DSKS’. The first is a good folder, constructed by a rank-ordering procedure

that assigns energies to contacts, and the second is a bad folder which has been first studied by Dinner et al. [11]. The values of the Gaussian contact energies have a mean of about -1 in both cases. The values of T_f and T_{min} are 1.15 and 1.2 for sequence A and 0.195 and 0.8 for DSKS'. The plot of t_{fold} vs. T for sequence A is shown in Figure 10. One reason to display it is that before no explicit care of the detailed balance condition has been made (which affects the low T branch of the curve somewhat). More importantly, the figure shows that the low temperature data agree with the Arrhenius law, $t_{fold} \sim \exp(\delta E/T)$ with δE of about 3.7.

The Arrhenius law has been obtained in the numerically exact studies of the 12-monomer sequences [8]. The barrier δE in that case has been associated with trajectories exiting from the most effective trap state and ending in the native state. What determines δE is the biggest single step energy cost on the trajectory with the smallest overall barrier. For the $N=16$ system A, we identify the trap state by studying the biggest occupancies of the local energy minima at temperatures 0.4 and 0.3. The three most heavily represented traps (denoted as TRAP 1, TRAP 2, and TRAP 3) are also shown in Figure 10, together with their corresponding δE 's. All three are displayed because the Monte Carlo data yield their occupancies to be of rather comparable values. The biggest δE , of 3.6263, is associated with TRAP 1 which explains the value found by fitting t_{fold} to the Arrhenius law. The other two traps have similar but smaller values.

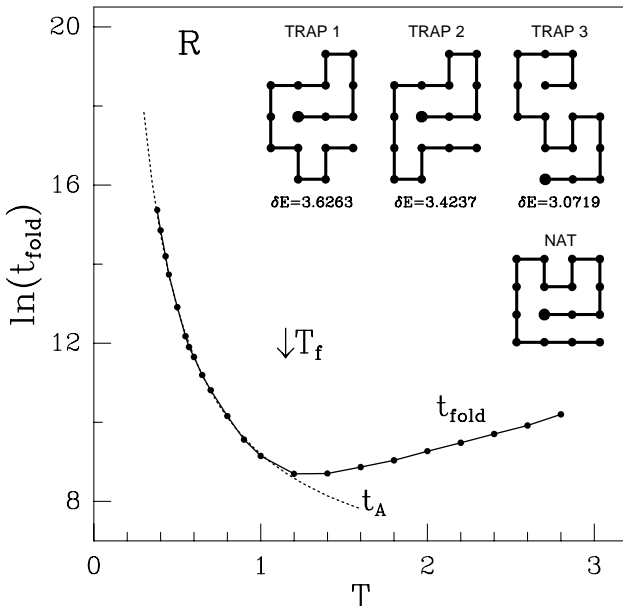


FIG. 10. Median folding time, based on 200 Monte Carlo trajectories, for the 16-monomer sequence R – the solid line. The dotted line corresponds to the Arrhenius law with $\delta E=3.7$. The conformations shown at the top are the three most relevant kinetic trap states. The corresponding values of δE are written underneath. The native conformation is denoted by NAT. The first bead is shown enlarged.

We now consider coarse graining of the dynamics. The results on the cell dynamics have been reported before [6,7] and here we focus only on the dynamics based on the LM's. Sequence R has 9103 LM's (out of which 2024 are U-shaped) and sequence DSKS' – 9424 (2253 U-shaped). We generate 200 Monte Carlo trajectories that we map to LM's by the steepest descent method. For each T we determine which of these LM's belong to the top 1000 in terms of their occupational probability. We then redo the runs and monitor connectivities between the 1000 LM's.

Figure 11 shows relevant portions of the connectivity graph for sequence R at $T=1.2$ and 2.0 whereas Figure 12 is for $T=0.8$ and 0.6. The two figures have been obtained by using a cutoff of 0.001 for a single connectivity line with a normalization in which all monitored connectivities add up to 1. The tree which could be interpreted as the folding funnel is most extended at $T=1.2$, i.e. for the most favorable folding conditions. This tree sheds its branches on going both to high and low temperatures. The transitions at low T span much smaller energies than at higher T 's. Furthermore, the low T non-native trees are quite elaborate. The looks of the low and high T graphs are quite distinct then and at T_{min} the features of the low and high T dynamics combine to generate an involved funnel of states.

Figure 13 shows the corresponding graphs for DSKS' at $T=1.2$ and 0.6. There is no tree of connections to the native state at any of these temperatures. Instead there are many disconnected clusters that cover small energy scales.

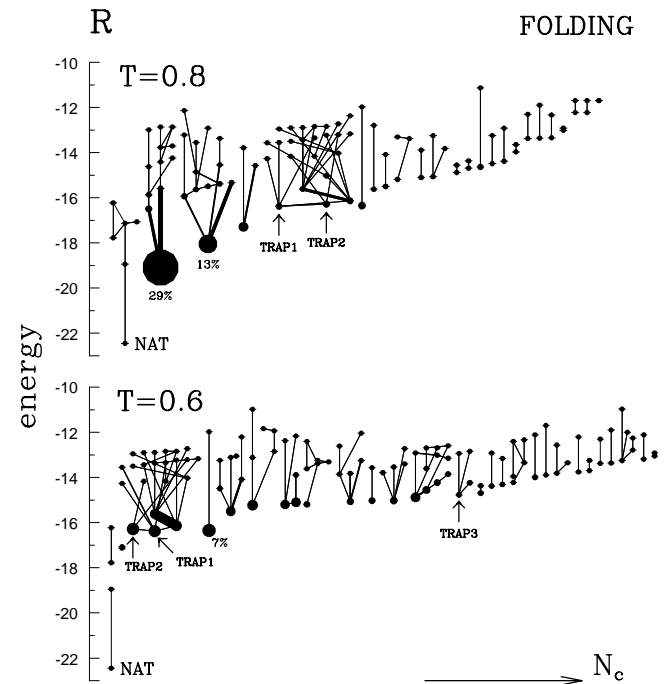


FIG. 11. Graph of connectivities for sequence R at $T=0.8$ and 0.6. The top figure shows 58% of all connectivities that were monitored and the bottom figure – 69%. Other connectivity graphs are not shown. The trap states are indicated.

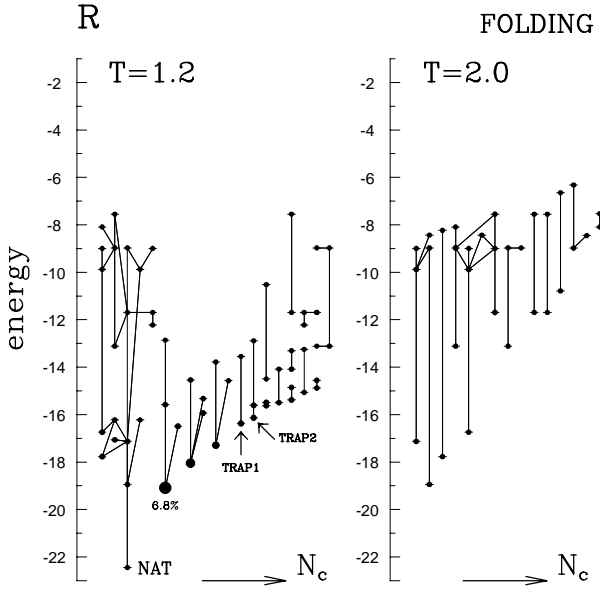


FIG. 12. Graph of connectivities for sequence R at $T=1.2$ and 2. The first shows 19% and the other 9% of the connectivities.

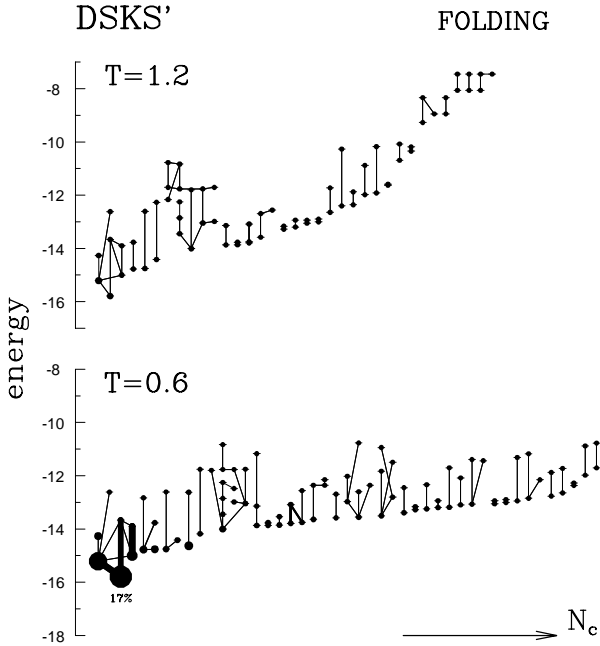


FIG. 13. Graph of connectivities for sequence DSKS'. For $T=1.2$ 18% of the connectivities are shown, whereas for $T=0.6$ - 71%.

III. 27-MONOMER SEQUENCE IN THREE DIMENSIONS

The problems of the state monitoring compound when working with heteropolymers in three dimensions. For a 27-monomer chain, such as considered by Sali et al. [12]

and Shrivastava et al. [13] one cannot even enumerate all local energy minima, except for those which are maximally compact, so we need a basis of states that relates only to the states encountered.

We have constructed a sequence, C, by generating the 156 contact energies from the Gaussian probability distribution with the mean of -2 and assigning them to the target shown in ref. [12]. The assignment has been done as follows: the values of contact energies were rank ordered and the strongest attracting couplings were allocated to the 28 contacts present in the $3 \times 3 \times 3$ target shape. The signs of the remaining non-native contact energies were modified so that 50% of them were attractive and 50% repulsive. This way of the sequence design has been demonstrated [13] as leading to the fastest folding characteristics. Our Monte Carlo based estimates for sequence C yield $T_f \approx 2.57$ and $T_{min} \approx 2.5$. At T_{min} , the median folding time is very short, for 3D sequences, – of order 45000 steps which minimizes the number of states to deal with.

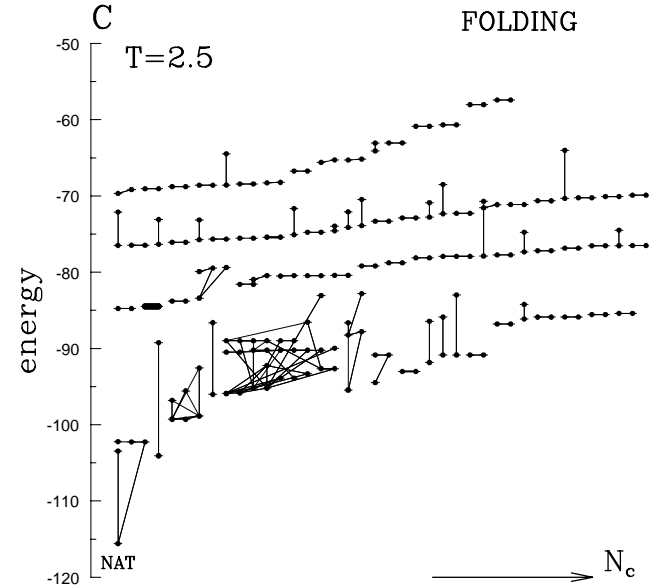


FIG. 14. Graph of connectivities for the three dimensional 27-monomer sequence C. The cutoff of adopted here is 0.0005. The basis of 1000 LM's used takes into account about 23% of the total Monte Carlo time.

In order to characterize the dynamics by the LM-based connectivity graphs we adopted the following procedure. First, we generated 100 folding trajectories at T_{min} and selected 30 of them which were the shortest. The steepest-descent-based mapping was then applied to the selected trajectories. For each of them, the number of LM's did not exceed 20 000. We worked with a temporary basis of 20 000 local minima from which low occupancy states were being removed during the process. The end result was to pick 1000 'finalists' – the LM's which were populated the most. The 30 runs were repeated again to determine the connectivities between the 1000 finalists.

These are shown in Figure 14. The LM-based dynamics is seen to be very fragmented with little structure which would be connected to the native state. It is possible that delineating a native knot - due to the enormous number of states - needs much more averaging over trajectories than the number we could study.

Therefore, we considered another approach in which we do not monitor the strengths of the connectivities but study the overlaps between the 30 trajectories, no matter how often a given link has appeared. The resulting graph of connectivities is shown in Figure 15. Here, we show only those links which have appeared in at least 4 trajectories which represents the dynamics in terms of 11 knots or clusters (there would be 45 clusters with the cutoff of 2). The native knot is tree-like and it has a substantial structure. This suggests that when too many states are involved, an overlap method of constructing the linkages may be preferable.

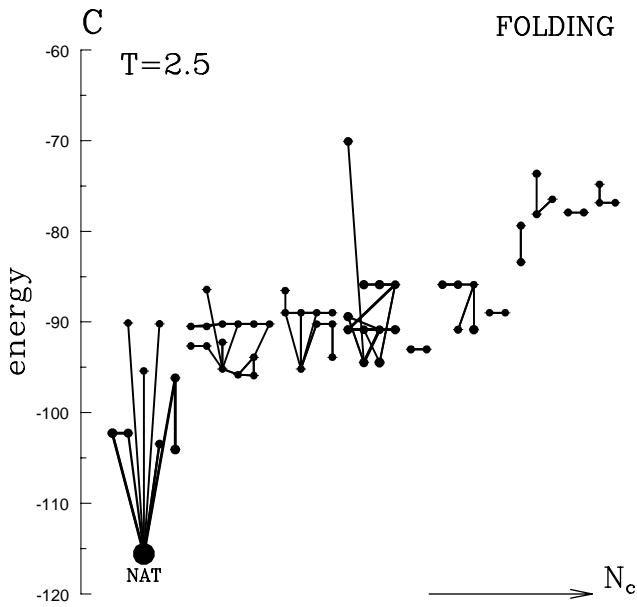


FIG. 15. Graph of connectivities for sequence C obtained by studying overlaps between the trajectories.

We conclude that the steepest-descent based dynamics does allow to distinguish between the good and bad folders. It provides a fairly detailed and meaningful representation of the dynamics, especially in the case of small two-dimensional systems. The connectivity patterns and the emergence of structures that can be identified with the folding funnel in good folders depend on the Hamiltonian, the adopted dynamics, and on the kind of the lattice used. Methods for three-dimensional heteropolymers need to be developed further. It is expected that the procedures proposed in our paper will be even more useful when applied to off-lattice 3D models. An alternative to the steepest descent based projection is to develop coarse-graining methods which are not based on the mapping to the local energy minima but instead, do

statistical analysis of features in the actual trajectories. For instance, in a recent publication [14], Du et. al. have proposed to measure kinetic distances between conformations of heteropolymers in terms of a ‘transition coordinate’ which is related to the probability to fold from a conformation without a preceding unfolding.

It is a pleasure to acknowledge many stimulating discussions with J. R. Banavar. Discussions with M. S. Li are also appreciated. This work was supported by KBN (Grant No. 2P03B-025-13).

- [1] K. A. Dill, S. Bromberg, S. Yue, K. Fiebig, K. M. Yee, D. P. Thomas, and H. S. Chan, *Protein Sci.* **4**, 561-602 (1995); C. J. Camacho and D. Thirumalai, *Proc. Natl. Acad. Sci. USA* **90**, 6369-6372 (1993); H. S. Chan and K. A. Dill, *Phys. Today* **46**, 24 (1993).
- [2] J. N. Onuchic, P. G. Wolynes, Z. Luthey-Schulten, *Proc. Natl. Acad. Sci.* **92**, 3626-3630 (1995); J. D. Bryngelson, J. N. Onuchic, N. D. Socci, and P. G. Wolynes, *Proteins: Struct. Funct. and Genet.* **21**, 167-195 (1995).
- [3] P. E. Leopold, M. Montal, and J. N. Onuchic, *Proc. Natl. Acad. Sci. USA* **89**, 8721-8725 (1992).
- [4] F. H. Stillinger and T. A. Weber, *Science* **225**, 2408-2416 (1983).
- [5] M. Cieplak and J. Jaeckle, *Z. Phys.* **66**, 325-332 (1987).
- [6] M. Cieplak, S. Vishveshwara, and J. R. Banavar, *Phys. Rev. Lett.* **77**, 3681-3684 (1996).
- [7] M. Cieplak and J. R. Banavar, *Folding & Design* **2**, 235-245 (1997).
- [8] M. Cieplak, M. Henkel, J. Karbowski, and J. R. Banavar, *Phys. Rev. Lett.* **80**, 3654 (1998).
- [9] N. D. Socci and J. N. Onuchic, *J. Chem. Phys.* **101**, 1519 (1994).
- [10] H. S. Chan and K. A. Dill, *J. Chem. Phys.* **100**, 9239-9257 (1994).
- [11] A. Dinner, A. Sali, M. Karplus, and E. Shakhnovich, *J. Chem. Phys.* **101**, 1444-1451 (1994).
- [12] A. Sali, E. Shakhnovich, and M. Karplus, *Nature* **369**, 248-251 (1994).
- [13] I. Shrivastava, S. Vishveshwara, M. Cieplak, A. Maritan, and J. R. Banavar, *Proc. Natl. Acad. Sci. U.S.A.* **90**, 9206-6372 (1995).
- [14] R. Du, V. S. Pande, A. Yu. Grosberg, T. Tanaka and E. S. Shakhnovich, *J. Chem. Phys.* **108**, 334-350 (1998)